Chloride-Modulated Insertion Reactions of Dimethylallene across the Pd−C Bond in Palladium Methyl Complexes Bearing Potentially Terdentate Pyridylthioether Ligands

Luciano Canovese,*,† Fabiano Visentin,† Gavino Chessa,† Paolo Uguagliati,† Claudio Santo,† Giuliano Bandoli,‡ and Lucia Maini§

Dipartimento di Chimica, Università Ca' Foscari, Calle Larga S. Marta 2137, 30123 Venezia, Italy, Dipartimento di Scienze Farmaceutiche, Università di Padova, Via F. Marzolo 5, 35131 Padova, Italy, and Dipartimento di Chimica "G. Ciamician", Università di Bologna, Via Selmi 2, 40126 Bologna, Italy

Received April 22, 2003

Palladium methyl complexes with potentially terdentate pyridylthioether (S−N−S(R) = 2,6-bis(R-thiomethyl)pyridine, R = Me, *t*-Bu, Ph; N−S−N = 2[(2-pyridylmethylthio)methyl]-pyridine) ligands have been prepared and characterized. Both the bidentate chloride [Pd(Me)(S−N−S(R))]Cl and the terdentate chloride-free [Pd(Me)(S−N−S(R))]$^+$ species are present in solution and display a substantially different reactivity toward allene insertion across the Pd−C bond. The structures of the complexes [Pd(Me)(S−N−S(*t*-Bu))]OTf and [Pd(Me)(S−N−S(*t*-Bu))]Cl were determined by X-ray diffraction. The chloride methyl substrates [Pd(Me)(S−N−S(R))]Cl display an enhanced reactivity in solution with respect to the allene insertion, and this reactivity was traced back to the distortion of the main coordination plane induced by the presence of an uncoordinated $-CH_2-S-R$ group in position 6 of the coordinating pyridine. The equilibrium position between the terdentate and the bidentate species can be modulated by addition of chloride ion, which therefore controls the overall reactivity of the system.

Introduction

The insertion reactions of unsaturated molecules into metal−carbon bonds are of widespread importance in numerous synthetic paths to C−C bond formation.[1] In particular palladium complexes are largely used in catalyzed copolymerization reactions leading to carbon monoxide, alkene, alkyne, and allene copolymers.[2] Moreover, the choice of the organometallic catalysts is of paramount importance in determining the reactivity and the regio-stereochemical features of the system under study. In this respect we have recently demonstrated that distortion of the flexible backbone of the ancillary ligands may induce a considerable increase in the rate of allene (1,1′-dimethylallene, DMA; 1,1′, 3,3′-tetramethylallene, TMA) insertion into the palladium−carbon bond in pyridylthioether halide methyl palladium complexes ([PdX(Me)(RN−SR′)], X = Cl, Br, I; R = H, Me, Cl; R′ = Me, *t*-Bu, Ph) to give the corresponding allyl complexes.[3] We decided to extend our mechanistic study to systems bearing potentially terdentate pyridylthioether species as ancillary ligands (S−N−S(R), N−S−N) since these ligands may impart a peculiar reactivity to their complexes. The complexes under study, the corresponding allyl species, and the atom-numbering scheme (which implies no isomeric preferences but indicates only atom location) are reported in Scheme 1.

In this respect several investigations were made by us and other authors,[4] and some interesting results were obtained. Thus, the palladium allyl derivatives of terdentate ligands display a facile room-temperature $\eta^3-\eta^1-\eta^3$ isomerism of the allyl fragment,[4c,d] and the Pd(0) olefin derivatives show a reactivity consistent with the capability of the terdentate ligand to stabilize Pd(0) three-coordinate species, thereby inducing a dissociative path parallel to the associative one in olefin exchange

* Corresponding author. E-mail: cano@unive.it.
† Università Ca' Foscari.
‡ Università di Padova.
§ Università di Bologna.

(1) (a) Shimuzu, I.; Tsuji, J. *Chem. Lett.* **1984**, 203. (b) Ahmar, M.; Caszes, B.; Goré, J. *Tetrahedron Lett.* **1984**, *25*, 4505. (c) Ahmar, M.; Caszes, B.; Barieux, J. J.; Goré, J. *Tetrahedron* **1987**, *43*, 513. (d) Cazes, B. *Pure Appl. Chem.* **1990**, *62*, 1867. (e) van Leeuwen, P. W. N. M.; van Koten, G. In *Catalysis: An Integrated Approach to Homogeneous, Heterogeneous and Industrial Catalysis*; Mouljin, J. A., et al., Eds.; Elsevier Science: Amsterdam, 1993 (and references therein). (f) Besson, L.; Gorè, J.; Cazes, B. *Tetrahedron Lett.* **1995**, *36*, 3853 and 3857. (g) Delis, J. G. P.; Aubel, P. G.; Vrieze, K.; van Leeuwen, P. W. N. M. *Organometallics* **1997**, *16*, 2948. (h) Kacker, S.; Sen, A. *J. Am. Chem. Soc.* **1997**, *119*, 1028. (i) Grigg, R.; Monteith, M.; Sridharan, V.; Terrier, C. *Tetrahedron* **1998**, *54*, 3885. (j) Zenner, J. M.; Larock, R. C.; *J. Org. Chem.* **1999**, *64*, 7312. (k) Yamamoto, A. *J. Chem. Soc., Dalton Trans.* **1999**, 1027. (l) Mecking, S. *Coord. Chem. Rev.* **2000**, *203*, 325 (and references therein). (m) Zimmer, R.; Dinesh, C. U.; Nandanan, E.; Khan, F. A. *Chem. Rev.* **2000**, *100*, 3067 (and references therein). (n) Yagyu, T.; Hamada, M.; Osakada, K.; Yamamoto, T. *Organometallics* **2001**, *20*, 1087. (o) Liu, W.; Malinoski, J. M.; Brookhart, M. *Organometallics* **2002**, *21*, 2836.

(2) Groen, J. H.; Elsevier, C. J.; Vrieze, K.; Smeets, W. J. J.; Spek, A. L. *Organometallics* **1996**, *15*, 3445 (and references therein)

(3) (a) Canovese, L.; Visentin, F.; Chessa, G.; Uguagliati, P.; Bandoli, G. *Organometallics* **2000**, *19*, 1461. (b) Canovese, L.; Visentin, F.; Chessa, G.; Santo, C.; Uguagliati, P.; Bandoli, G. *J. Organomet. Chem.* **2002**, *650*, 43. (c) Canovese, L.; Chessa, G.; Santo, C.; Visentin, F.; Uguagliati, P. *Inorg. Chim. Acta* **2003**, *346*, 158.

10.1021/om030293f CCC: $25.00
Publication on Web 06/24/2003

Scheme 1

S-N-S(R) Complexes

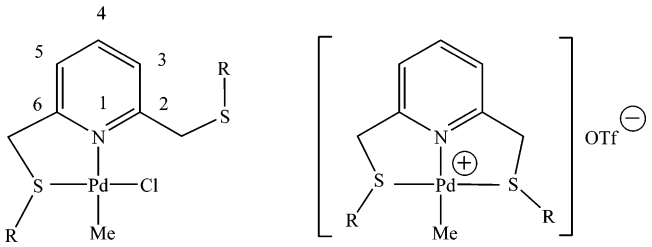

1a (R = Me)
1b (R =t-Bu)
1c (R = Ph)

2a (R = Me)
2b (R =t-Bu)
2c (R = Ph)

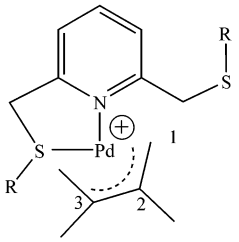

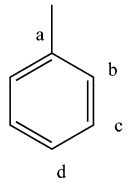

Phenyl group labelling scheme

3a (R = Me)
3b (R =t-Bu)
3c (R = Ph)

N-S-N Complexes

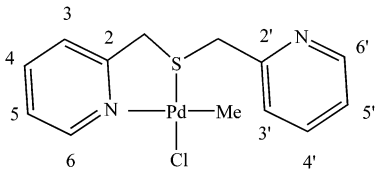

4

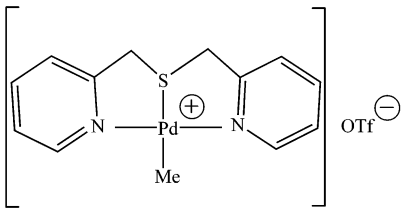

5

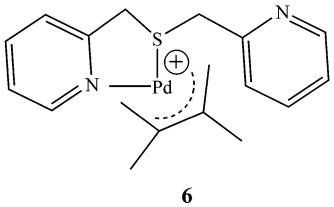

6

reactions;[4e] both these phenomena are promoted by the alternating attack of the third coordinating atom of the dangling wing of the ligand. In the case of methyl complexes, the presence of a potentially coordinating arm in position 6 of the pyridine ring of the ancillary ligand may induce distortion if uncoordinated or make

Scheme 2

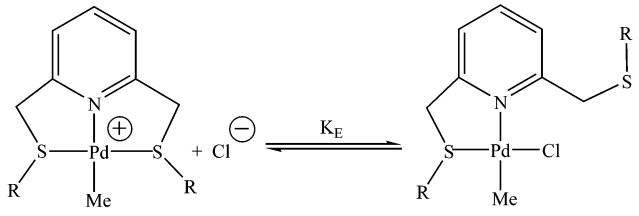

I *II*

the ligand act as a truly tris-chelating one, in any case influencing the stability of the ensuing allyl complex. Therefore, it appears that the presence of chloride ion could modulate the reaction rate of allene insertion by modifying the equilibrium position in Scheme 2,

where the tris-chelate complex **I** would display a decreased reactivity with respect to the bis-chelate **II** since the latter should resemble the most reactive 6-substituted species.[3] Thus, we decided to synthesize and study the complexes reported in Scheme 1, to assess their behavior in solution and their reactivity with respect to DMA insertion into the Pd−C bond in the presence (or in the absence) of free chloride ion. The results of such an investigation are reported in the present paper.

Result and Discussion

Synthesis of Palladium Complexes. Addition under inert atmosphere (N_2) of the potentially terdentate ligand L−L′−L (L−L′−L = S−N−S(R), N−S−N) to a solution of [PdCl(Me)(COD)] in THF yields the pyridylthioether methyl complex [Pd(Me)(L−L′−L)]Cl as air-stable yellow microcrystals.. These substrates were obtained in quantitative yields and are easily characterized by comparison of their ^{1}H NMR spectra with those of the corresponding free ligand. In fact the ^{1}H NMR spectra of the coordinated ligands display a generalized downfield shift of characteristic signals (i.e., $\Delta\delta_{CH2S(SNS)} = 0.8-1$, $\Delta\delta_{CH2S(NSN)} = 0.4$ ppm). Dechloridation of these species by AgOTf in CH_2Cl_2 and addition of diethyl ether to the filtered and concentrated reaction mixture yield the corresponding whitish ionic complexes [Pd(Me)(L−L′−L)]$^+$OTf$^-$. These substrates are air-stable microcrystalline species, and their solution behavior and consequently their ^{1}H NMR spectra are well differentiated from the corresponding chloride species (vide infra). The allyl derivatives were synthesized by the usual procedure starting from the corresponding allyl dimers by addition of the appropriate L−L′−L ligand [4d] or by reacting the chloro methyl palladium complexes with DMA.

Crystal Structure Determination. The ORTEP[5] drawing of the complex [Pd(Me)(S−N−S(*t*-Bu))]OTf is

(4) (a) Wehman, P.; Rülke, R. E.; Kaasjager, V. E.; Kamer, P. C. J.; Kooijman, H.; Spek, A. L.; Elsevier, C. J.; Vrieze, K.; van Leeuwen, P. W. N. M. *J. Chem. Soc., Chem. Commun.* **1995**, 331. (b) Rülke, R. E.; Kaasjager, V. E.; Wehman, P.; Elsevier, C. J.; van Leeuwen, P. W. N. M.; Vrieze, K.; Fraanje, J.; Goubitz, K.; Spek, A. L. *Organometallics* **1996**, *15*, 3022. (c) Canovese, L.; Visentin, F.; Uguagliati, P.; Chessa, G.; Lucchini, V.; Bandoli, G. *Inorg. Chim. Acta* **1998**, *275*, 385. (d) Canovese, L.; Visentin, F.; Chessa, G.; Niero, A.; Uguagliati P. *Inorg. Chim. Acta* **1999**, *293*, 44. (e) Canovese, L.; Visentin, F.; Chessa, G.; Gardenal, G.; Uguagliati, P. *J. Organomet. Chem.* **2001**, *622*, 155.

(5) Johnson, C. K. *ORTEP*, report ORNL-5138; Oak Ridge National Laboratory: Oak Ridge, TN, 1976.

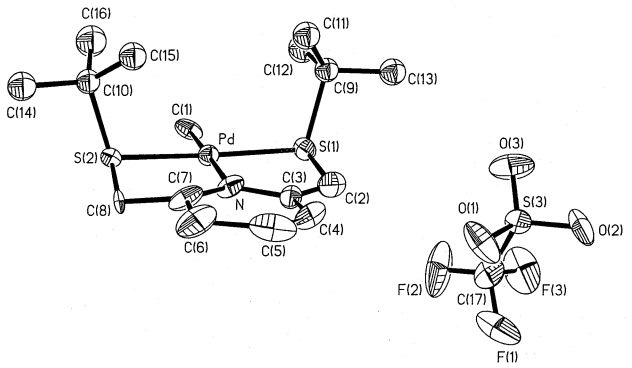

Figure 1. Drawing of the complex [Pd(Me)(S−N−S(*t*-Bu))]OTf (**2b**) with the numbering scheme. Ellipsoids are at the 40% level.

Table 1. Selected Bond Lengths (Å), Angles (deg), and Geometry of the Possible Weak Hydrogen Bonds for the Complex [Pd(Me)(S−N−S(*t*-Bu))]OTf

Bond Lengths			
Pd−S(1)	2.281(6)	Pd−S(2)	2.315(6)
Pd−N	2.078(6)	Pd−C(1)	2.079(8)
S(1)−C(2)	1.74(1)	S(2)−C(8)	1.92(2)
S(1)−C(9)	1.90(2)	S(2)−C(10)	1.85(1)
Bond Angles			
S(1)−Pd−N	83.5(6)	S(2)−Pd−N	88.6(6)
S(1)−Pd−C(1)	90.3(8)	S(2)−Pd−C(1)	97.6(8)
S(1)−Pd−S(2)	170.7(1)	N−Pd−C(1)	173.6(9)
Pd−S(1)−C(2)	100.7(5)	Pd−S(2)−C(8)	93.3(6)
S(1)−C(2)−C(3)	114.2(9)	S(2)−C(8)−C(7)	119(1)
C(2)−C(3)−N	118(1)	C(8)−C(7)−N	117(1)

Hydrogen Bonds			
D−H- - -A	H- - -A (Å)	D- - -A (Å)	D−H- - -A (Å)
C(2)−H(2a)- - -F(2)	2.61	3.45	145
C(8)−H(8a)- - -O (3A)[a]	2.65	3.52	151
C(8)−H(8b)- - -F (3A)[a]	2.64	3.35	130

[a] Refers to the atom in the position x, $1+y$, z.

shown in Figure 1, together with the numbering scheme used, while relevant bond lengths and angles are reported in Tables 1and 2. As can be seen in Figure 1, the "inner core" of the cation is roughly planar with S(1), S(2), C(9), and C(10) atoms above the average coordination plane (by 0.08, 0.15, 1.84, and 1.94 Å, respectively) and the C(2) and C(8) atoms below this plane (by 1.14 and 0.25 Å, respectively). The five-membered ring Pd−S(1)−C(2)−C(3)−N adopts a slightly envelope conformation with Pd, C(2), C(3), and N coplanar, whereas S(1) lies off by 0.20 Å. On the contrary, the Pd−S(2)−C(8)−C(7)−N ring shows a more pronounced envelope conformation with the C(8) atom out (by 0.38 Å) from the mean plane defined by Pd, S(2), C(7), and N atoms.

The Pd−S(1), Pd−S(2), and Pd−N distances (2.281(6), 2.315(6), and 2.078(6) Å, respectively) are in good agreement with the average values, retrieved from the Cambridge Structural Database,[6] in 39 mononuclear Pd(II) complexes for Pd−S distances (mean value: 2.306 Å) and in 23 cationic complexes containing Pd(II)−N (pyridine-type) bonds (mean value: 2.057 Å). Incidentally, the Pd(II)−N distance in neutral pyridine complexes rises to 2.162(5) Å, as can be noticed in numerous

(6) Allen, F. H.; Davies, J. E.; Gralloy, J. J.; Johnson, O.; Kennard, O.; Macrae, C. F.; Mitchell, E. M.; Mitchell, G. F.; Smith, J. M.; Watson, D. G. J. *Chem. Inf. Comput. Sci.* **1991**, *31*, 187; Cambridge Crystallographic Database (Version 5.22 of October 2001).

Table 2. Selected Bond Lengths (Å), Angles (deg), and Geometry of the Possible Weak Hydrogen Bonds for the Complex [Pd(Me)(S−N−S(*t*-Bu))]Cl

Bond Lengths			
Pd(1)−C(16)	2.034(6)	Pd(1−S(1)	2.2911(11)
Pd(1)−N(1)	2.074(4)	Pd(1)−S(2)	2.3029(12)
C(6)−S(1)	1.822(5)	C(11)−S(2)	1.792(6)
C(7)−S(1)	1.864(5)	C(12)−S(2)	1.859(5)
Bond Angles			
N(1)−Pd(1)−S(1)	85.63(10)	N(1)−Pd(1)−S(2)	85.70(10)
C(16)−Pd(1)−S(1)	93.36(18)	C(16)−Pd(1)−S(2)	95.24(18)
S(1)−Pd(1)−S(2)	170.46(5)	C(16)−Pd(1)−N(1)	178.6(2)
C(6)−S(1)−Pd(1)	96.82(14)	C(11)−S(2)−Pd(1)	98.14(17)
C(5)−C(6)−S(1)	115.0(3)	C(1)−C(11)−S(2)	117.6(4)
N(1)−C(5)−C(6)	116.1(4)	N(1)−C(1)−C(11)	117.8(5)

Hydrogen Bonds			
D−H- - -A	H- - -A (Å)	D- - -A (Å)	D−H- - -A (Å)
C(20)−H(20A)- - -Cl(2)	2.66	3.608(6)	166
C(21)−H(21A)- - -Cl(2)[a]	2.60	3.536(4)	163
C(21)−H(21B)- - -Cl(2)[b]	2.60	3.536(4)	163

[a] Refers to the atom in the position $-x$, $-y$, $-1-z$. [b] Refers to the atom in the position x, $-y$, $1/2+z$.

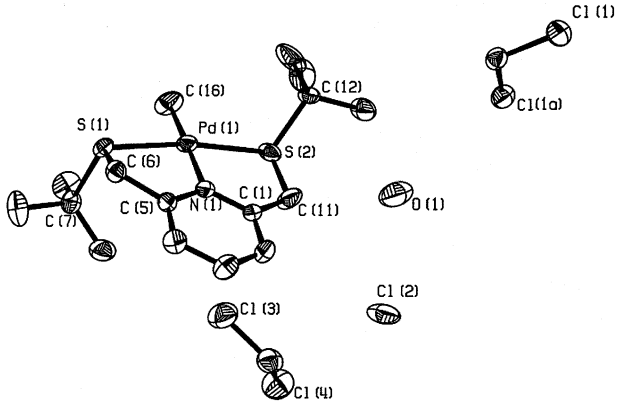

Figure 2. Drawing of the complex [Pd(Me)(S−N−S(*t*-Bu))]Cl (**1b**) with the numbering scheme. Ellipsoids are at the 40% level.

examples.[3a,b,7] No effective hydrogen bonds occur, and the complex is built up by juxtaposition at van der Waals distances of well-separated Pd(II) cations and sulfonate counteranions, although the separations involving the methylene hydrogens (Table 1a) seem to be of some significance.

We have also carried out the X-ray structure determination of the complex [Pd(Me)(S−N−S(*t*-Bu))]Cl, which apparently separates due to solubility factors from a CH_2Cl_2/hexane solution in which both species [PdCl(Me)(S−N−S(*t*-Bu))] and [Pd(Me)(S−N−S(*t*-Bu))]Cl are present in equilibrium. The ORTEP[5] drawing of the latter is shown in Figure 2, together with the numbering scheme used, while relevant bond lengths and angles are reported in Table 2.

[Pd(Me)(S−N−S(*t*-Bu))]Cl proved to be the *RS* isomeric form (the *tert*-butyl groups are located over and under the plane formed by the metal and the coordinating atoms). The coordination around the Pd(II) is analogous to the previously described complexes with

(7) (a) Kay, Y.; Yasuoka, N.; Kasay, N. *Bull. Chem. Soc. Jpn.* **1979**, *52*, 737. (b) Okeya, S.; Kawakita, Y.; Matsumoto. S.; Nakamura, Y.; Kawaguchi, S.; Kanehisa, N.; Miki, K.; Kasay, N. *Bull. Chem. Soc. Jpn.* **1981**, *55*, 2134. (c) Newkome, G. R.; Kiefer, G. E.; Frere, Y. A.; Onishi, M.; Gupta, V. K.; Fronczek, F. R. *Organometallics* **1986**, *5*, 348.

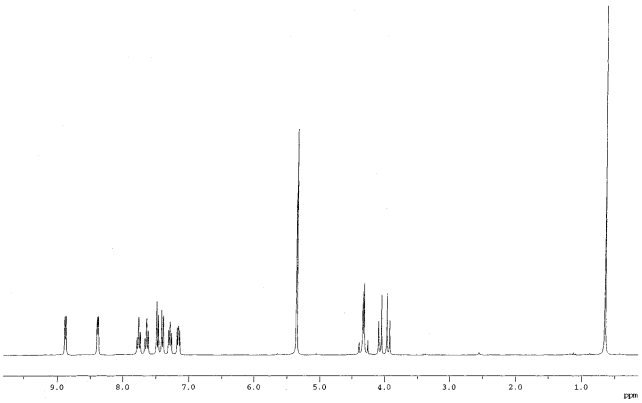

Figure 3. Low-temperature (203 K) ^{1}H NMR spectrum of the complex [PdCl(Me)(N−S−N)] (**4**) in CD_2Cl_2.

Pd(1)−S(1), Pd(1)−S(2), Pd(1)−N(1), and Pd(1)−C(16) distances of 2.2911(11), 2.3029(12), 2.074(4), and 2.034(6) Å, respectively. Both five-membered rings Pd(1)−S(1)−C(6)−C(5)−N(1) and Pd(1)−S(2)−C(11)−C(1)−N(1) adopt an envelope conformation with S(1) and S(2) placed at −0.46 and 0.24 Å with respect to the mean plane defined by Pd, C, and N atoms. One-half water molecule is present per formula unit; the water molecule forms two hydrogen bonds with the chloride atom (O- - -Cl^- distances 3.151(9) and 2.857(9) Å). The chloride atom interacts with the hydrogen atoms to form weak hydrogen bonds (Table 2).

Solution Behavior. [Pd (Me)(S−N−S(R))]Cl. The chloride methyl complexes (**1**) bearing the 2-bis(thiomethyl)pyridine derivatives S−N−S(R) as ancillary ligands behave differently from the corresponding N−S−N complex (**4**). The low-temperature ^{1}H NMR spectrum of the latter can be interpreted as arising from a truly arm-off species in which only two of the three potentially coordinating nucleophiles are coordinated to palladium. In fact, as can be seen in Figure 3, the presence of two different groups of signals in the aromatic zone and the two AB systems (at 4−4.5 ppm) ascribable to the diastereotopic CH_2−S−CH_2 protons contiguous to the chiral coordinated sulfur clearly support this hypothesis.

Apparently, the sp^3 sulfur hybridization disfavors the concomitant formation of two strained chelating rings. On the contrary, when the S−N−S derivatives **1** are studied, a general fluxionality ascribable to the alternating ligand wings movement is detectable at any attainable temperature. The thioetheric sulfurs of the S−N−S moiety can evidently act as efficient nucleophiles thanks to the flexibility of the backbone structure of the ligand itself and to the presence of two sp^3-hybridized sulfur atoms. Thus, the incoming sulfur linked to the joined uncoordinated wing can easily attack the metal center, thereby promoting the subsequent release of its symmetric counterpart. Under these circumstances the absolute sulfur configuration would rapidly interconvert and no diastereotopic protons would be detected. However, the case of the complex [Pd(Me)-(S−N−S(*t*-Bu))]Cl (**1b**) is peculiar in some respect. The low-temperature (188 K) ^{1}H NMR spectrum of the sample in CD_2Cl_2 (Figure 4) displays signals indicating the presence of one single species and one single well-resolved AB system at ca. 5 ppm ascribable to CH_2S protons. The formation of a symmetric pentacoordinate

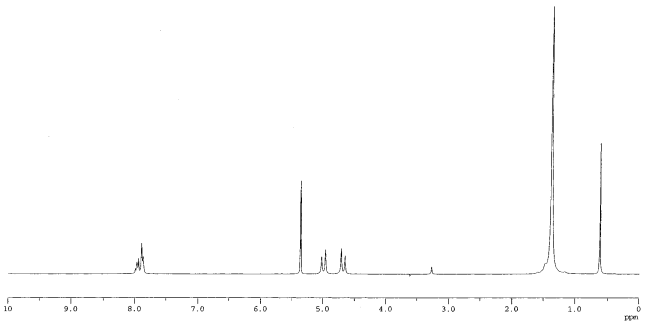

Figure 4. Low-temperature (188 K) ^{1}H NMR spectrum of the complex [PdCl(Me)(S−N−S(*t*-Bu))] (**1b**) in CD_2Cl_2.

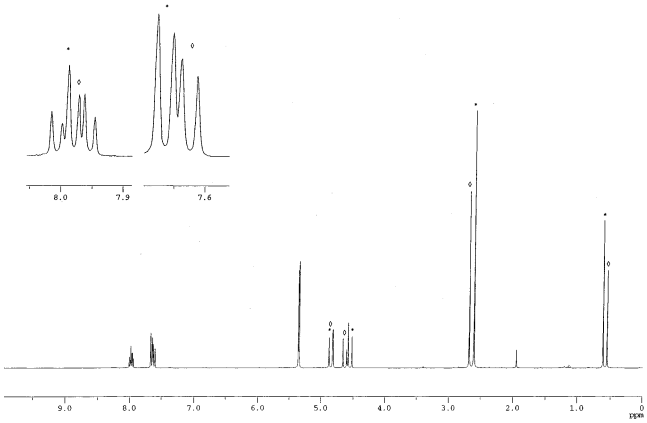

Figure 5. Low-temperature (223 K) ^{1}H NMR spectrum of the complex [Pd(Me)(S−N−S(Me))]OTf (**2a**) in CD_2Cl_2.

species promoted by the enhanced nucleophilicity of the *t*-Bu-substituted sulfur atoms should explain the observed behavior.

As an alternative explanation one should take into account a fast alternating coordination of the ligand wings without concomitant inversion of the sulfur absolute configuration. In other words, this movement is sterically controlled since the bulkiness of the *t*-Bu groups governs the enantiospecificity of the exchanging movement, with the configuration of sulfur lying on the incoming wing being somehow predetermined by that of the coordinated one.

[Pd(Me)(S−N−S(R))]OTf. The chloride-free complexes of S−N−S ligands (**2**) display a solution behavior typical of tercoordinated chelating ligands. The room-temperature NMR spectra display symmetric structures in which the rapid inversion of the absolute sulfur configuration is the only observable fluxionality. At low temperature the sulfur inversion is frozen and the ^{1}H NMR spectra display the presence of a pair of diastereoisomers (*meso* and *RS*) in different populations together with the AB systems of the endocyclic CH_2S protons. The low-temperature spectrum (208 K) of the complex [Pd(Me)(S−N−S(*t*-Bu))]$^+$ (**2b**) displays the presence of almost only one isomer (∼90%), the isomeric distribution at 223 K for the other complexes being ∼60% (R = Me (**2a**)) (Figure 5), ∼70% (R = Ph (**2c**)).

The room-temperature ^{1}H NMR spectrum of [Pd(Me)-(N−S−N)]$^+$ (**5**) exhibits signals that clearly belong to a truly tercoordinate species. However, several broad signals observed in the spectrum suggest the presence of oligo- or polymeric structures. These oligomers, probably due to the distorted third arm of the ligand

Scheme 3

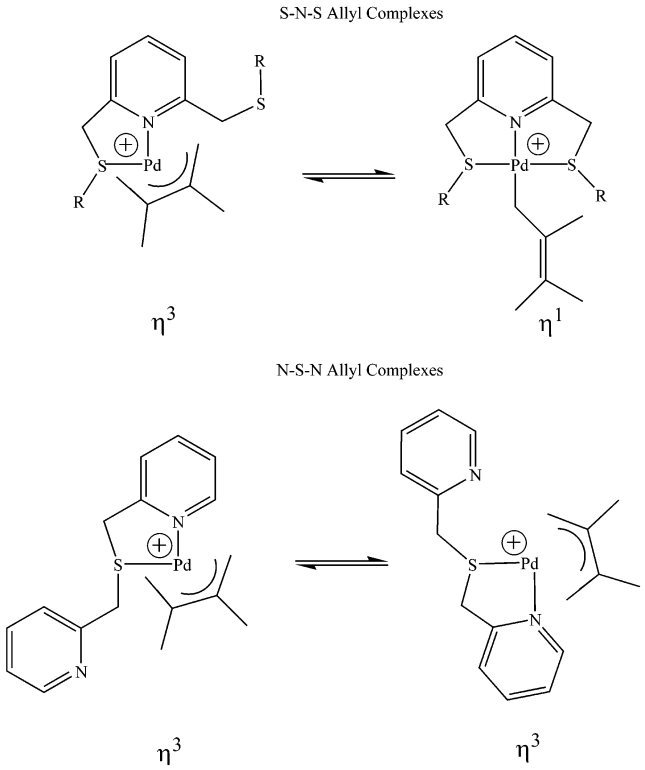

Scheme 4

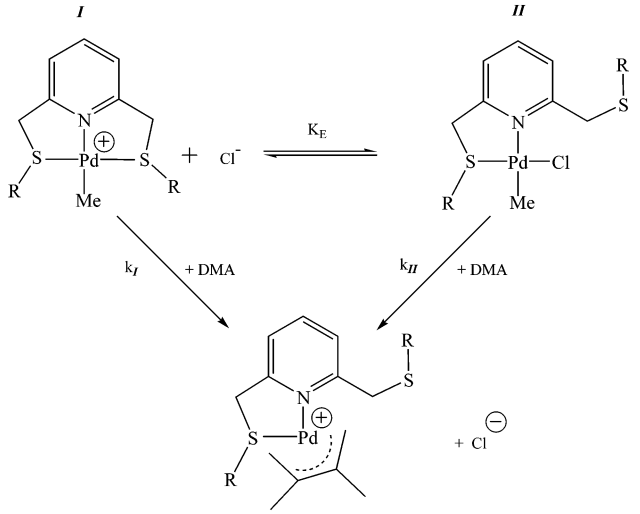

interfering with adjacent molecules, behave as the monomeric species when reacting with DMA, giving rise quantitatively to the expected allyl complex (**6**).

As for the allyl complexes, they do not deserve a detailed description since their solution behavior is quite similar to that of analogous species described by us elsewhere.[4d,8] It should be sufficient to recall that complexes bearing asymmetric allyl fragments and a potentially tercoordinate ligands (although they should exist as four diastereoisomers owing to the presence of the asymmetric uncoordinated wing) rapidly interconvert at room temperature. The fast fluxional rearrangement observed is due to the $\eta^3-\eta^1-\eta^3$ isomerism of the allyl fragment induced by the nucleophilic attack of the uncoordinated sulfur on the dangling wing. Under these circumstances the sulfur absolute configuration inversion remains obviously operative. On the contrary, the N−S−N ligand, although undergoing the fast alternating coordination movement, never induces $\eta^3-\eta^1-\eta^3$ isomerism, and the low-temperature (223 K) ^{1}H NMR spectrum shows the presence of a substrate in which the ligand acts like a bidentate (Scheme 3).

Sulfur inversion is "frozen" in this case, and a pair of AB systems ascribable to $H_2C-S-CH_2$ protons are observed which arise from the position of the substituted allyl terminus with respect to the uncoordinated or to the coordinated wing.[4d] However, only one species among the four possible diastereoisomers is detectable under our experimental conditions, which should originate from an asymmetric ligand (bidentate N−S−N) coupled with an asymmetric allyl fragment. In this case, the less energetic process is probably the alternating attack of the dangling pyridines, which goes on despite the low temperature. However, since only one species is detectable, we may conclude either that more likely the sulfur freezes into only one preferential configuration (only one diastereoisomer and its undetected enantiomer) or that the two diastereoismers are isochronous. These processes are clearly attributable to the peculiar configuration of the N−S−N ligand, which disfavors concomitant formation of two strained rings, which in turn should induce the $\eta^3-\eta^1-\eta^3$ allyl isomerism.

Kinetics and Mechanism of the Allene Insertion Reaction. From NMR data it appears that in the case of S−N−S derivatives the chloride complexes (**II**) react considerably faster than their chloride-free counterparts (**I**). In fact the chloride derivatives react almost instantaneously, whereas the reaction involving the chloride-free substrates takes several hours under NMR experimental conditions (vide infra).

However both **I** and **II** species react with allene; thus the chloride concentration is time dependent and therefore it can modulate the equilibrium position and consequently the observed rate constant in such a way as to make its determination not straightforward (Scheme 4).

The kinetic Scheme 4 could in principle be easily integrated numerically as a function of the parameters $k_{\mathbf{I}}$, $k_{\mathbf{II}}$, and K_{E}. These can be determined by UV/vis spectrophotometry via nonlinear regression of absorbance to time data. However, owing to the high parameter correlation, the close proximity of extinction coefficients of **I** and **II**, and the high difference between $k_{\mathbf{I}}$ and $k_{\mathbf{II}}$ (vide infra), we preferred to dissect the overall kinetic study into partial, separate sections corresponding to (i) direct determination of K_{E}, (ii) independent determination of $k_{\mathbf{I}}$ (from the chloride-free species **I** in the absence of added Cl^-), and (iii) independent determination of $k_{\mathbf{II}}$ starting from **II** in the presence of an excess of Cl^-. The resulting data are reported in Table 3.

The equilibrium constants K_{E} were determined by ^{1}H NMR technique by adding successive aliquots of triethylbenzylammonium chloride (TEBA) to a CD_2Cl_2 solution of substrate **I** ($[Pd]_0 \approx 10^{-2}$ mol dm^{-3}; the ionic strength was not controlled) and recording the resulting spectrum at 298 K (see Experimental Section and Figure 6).

(8) Canovese, L.; Visentin, F.; Uguagliati, P.; Lucchini, V.; Bandoli, G. *Inorg. Chim. Acta* **1998**, *277*, 247.

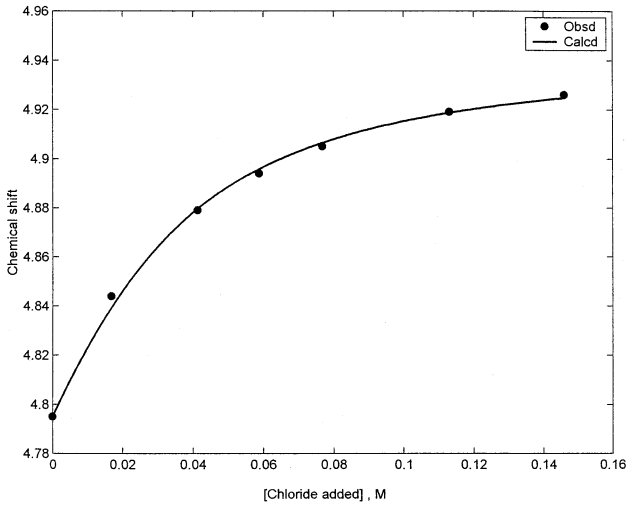

Figure 6. ^{1}H NMR chemical shift changes (298 K) upon addition of triethylbenzylammonium chloride to a CD_2Cl_2 solution of [Pd(Me)(S−N−S(Me))]OTf (**2a**). Solid line is the best-fitting curve according to the model (see Experimental Section).

The final ^{1}H NMR spectrum ($[Cl^-]_0 \approx [Pd]_0$) was virtually superposable to that of an authentic sample of chloride species **II**. The equilibrium constants (Table 3) reflect the nucleophilic capability of the R-substituted sulfur (the S−N−S(Ph) ligand being the less coordinating species and the S−N−S(*t*-Bu) the more coordinating one). Despite the high nucleophilic strength of Cl^- in nonprotic solvents, no hints of complete displacement of the ligands were observed. Apparently, the chelating effect of the terdentate species is overwhelmed by the chloride only when the mutual *trans*-influence of the *trans*-coordinated chalcogen atoms is operative.

The chloride-free complexes **I** react slowly with DMA, whose insertion into the Pd−Me bond was directly determined by ^{1}H NMR technique under second-order conditions (following the methyl signal disappearance) only in the case of the species $[Pd(Me)(S-N-S(Ph))]^+$ (**2c**). The substrates $[Pd(Me)(S-N-S(R))]^+$ (**2a**, **2b**) are much less reactive, and in both cases the rate constant was deduced from the half-life of the reaction (Table 2). According to all the previous findings,[3] the associative attack of allene on the metal center is disfavored by increasing basicity of the sulfur and by increasing steric requirements of the substituent R of the sulfur itself. However, the most noticeable result is the difference between the rate constants of the chloride-free (**I**) and the chloride (**II**) substrates (Table 2), which span several orders of magnitude. The chloride species **II** behave similarly to the bidentate pyridylthioether chloro methyl complexes bearing a substituent group (Me, Cl) in position 6 of the pyridine ring. Since the high reactivity of the latter species was traced back to the distortion of the chelate ring with respect to the main coordination plane,[3] we therefore advance the hypothesis that the uncoordinated wing would induce an analogous effect. Thus the chloride ion can modulate the overall rate of allene insertion by simply modifying the position of equilibrium between the closed (**I**) and the partially open (**II**) species. Moreover, it was demonstrated[3b,c] that the reactivity in this type of reaction depends strongly on the basicity of the pyridine nitrogen, which can be varied by changing the electronegativity of the 6-substituent. Thus, since the electron-withdrawing capability of the CH_2−Py group lies between those of Me and Cl^- groups, the ensuing reactivity of the bis-chelate chloride substrates (**II**) appears reasonable since it is intermediate between those of the bidentate pyridylthioether substrates bearing chloride and a methyl group in position 6 of the pyridine ring.

Curiously both the complexes derived from the N−S−N ligand (chloride and chloride-free) behave differently from the corresponding S−N−S species. When DMA is added to a CD_2Cl_2 solution of the chloride-free substrate, an immediate reaction is observed. The typical ^{1}H NMR spectrum of the corresponding allyl derivative quantitatively formed suggests that the substrate reacts irrespectively of its mono- or oligomeric form and that the reaction is fast, analogously to those where bidentate solvento substrates are involved;[3c] on the other hand, the reactivity of the chloride species is independent of added chloride. Apparently the poorly coordinating pyridine nitrogen of the arm-off wing (vide supra) does not displace the chloride ion, thereby imparting to the N−S−N derivatives a low reactivity analogous to that of an authentic bis-chelate chloride species. As a matter of fact, since the structure of the latter in solution is not distorted (the coordinated pyridine ring is not substituted in position 6), its reactivity lies between those of the bidentate HN−SPh and HN−SMe chloro-methyl derivatives (Table 3).

Experimental Section

Terdentate Ligands. 2-[(2-Pyridylmethylthio)methyl]-pyridine (N−S−N) and 2,6-bis(R-thiomethyl)pyridine (S−N−S(R); R= Me, *t*-Bu, Ph) were synthesized according to published procedures.[4c−e] All solvents were purified and distilled by standard methods before use, while all other analytical grade reagents were used as received.

[PdCl(Me)(COD)]. The title complex was obtained from $[Pd(COD)Cl_2]$[9] following the published procedure.[10]

[Pd(Me)(S−N−S(Me))]Cl (1a). To a solution of 226.3 mg (1.14 mmol) of 2,6-bis(mehtylthiomethyl)pyridine (S−N−S(Me)) in 20 mL of THF was added 273.6 mg (1.03 mmol) of [PdCl(Me)(COD)]. The solution was stirred for 4 h, although the reaction product starts precipitating after 1 h owing to its low solubility in THF. The reaction mixture was dried under reduced pressure and dissolved in 15 mL of CH_2Cl_2, treated with activated charcoal, filtered on Celite filter, and reduced to a small volume. Addition of diethyl ether yields a yellowish oily product, which was crystallized by stirring at 0 °C. The yellow microcrystals were filtered off, washed with 20 mL of diethyl ether, and dried under vacuum (334.8 mg, 91%). ^{1}H NMR ($CDCl_3$, T = 298 K, ppm): pyridine protons δ 7.93 (m, 3H, H^3_{Pyr}, H^4_{Pyr}, H^5_{Pyr},), thiomethyl protons δ 5.04 (s, 4H, Pyr(CH_2−S)$_2$), methyl protons δ 2.75 (s, 6H, S−CH_3), methyl protons δ 0.63 (s, 3H, Pd−CH_3). IR: $\nu_{C=N}$ 1595.1 cm^{-1} (KBr). Anal. Calcd for $C_{10}H_{16}ClNPdS_2$: C, 33.71; H, 4.53; N, 3.93. Found: C, 33.50; H, 4.64; N, 3.68.

The following complexes were synthesized in the same way as [Pd(Me)(S−N−S(Me))]Cl using the appropriate ligand.

[Pd(Me)(S−N−S(*t*-Bu))]Cl (1b). Yield: 92% (yellow microcrystals). ^{1}H NMR ($CDCl_3$, 295 K, ppm): pyridine protons δ 8.09 (2H, H^3_{Pyr},H^5_{Pyr}, d, J = 7.7 Hz), 7.92 (t, 1H, H^4_{Pyr}, J = 7.1 Hz), thiomethyl protons δ 4.99 (s, 4H, Pyr-CH_2−S), *tert*-butyl protons δ 1.49 (s, 18H, S−C(Me)$_3$), methyl protons δ 0.74 (s,

(9) Chatt, J.; Vallarino, L. M.; Venanzi, L. M. *J. Chem Soc.* **1957**, 3413.

(10) Rülke, R. E.; Ernsting, J. M.; Spek, A. L.; Elsevier, C. J.; van Leeuwen, P. W. N. M.; Vrieze, K. *Inorg. Chem.* **1993**, *32*, 5769.

3H, Pd−CH_3). IR: $\nu_{C=N}$ 1597.0 cm^{-1} (KBr). Anal. Calcd for $C_{16}H_{28}ClNPdS_2$: C, 43.64; H, 6.41; N, 3.18. Found: C, 43.88; H, 6.25; N, 3.32.

[Pd(Me)(S−N−S(Ph))]Cl (1c). Yield: 94% (yellow microcrystals). ^{1}H NMR ($CDCl_3$, 298 K, ppm): pyridine and phenyl protons δ 7.75−7.47 (m, 5H, H^4_{Pyr}, H_{meta}), δ 7.30, (m, 8H, H^5_{Pyr}, H^3_{Pyr}, H_{ortho}, H_{para}), thiomethyl protons δ 5.03 (s, 4H, Pyr−CH_2−S), methyl protons δ 1.10 (s, 3H, Pd−CH_3). ^{13}C NMR (in $CDCl_3$, 298 K, ppm): pyridine carbons δ 157.45 (C^2_{Pyr}, C^6_{Pyr}), 138.38 (C^4_{Pyr}), 122.88 (C^3_{Pyr}, C^5_{Pyr}), phenyl carbons δ 131.73, 129.21, 128.90, thiomethyl carbons δ 47.57 (S−CH_2−Pyr), methyl carbons δ −5.32 (Pd−CH_3). IR: $\nu_{C=N}$ 1597.0 cm^{-1} (KBr). Anal. Calcd for $C_{20}H_{28}ClNPdS_2$: C, 50.00; H, 4.20; N, 2.92. Found: C, 49.74; H, 4.28; N, 2.93.

[PdCl(Me)(N−S−N))] (4). Yield: 91% (red-brown microcrystals). ^{1}H NMR ($CDCl_3$, 298 K, ppm): pyridine protons δ 8.74 (bs, 2H, H^6_{Pyr}) 7.69 (Td, 2H, H^4_{Pyr} J = 7.7 Hz, J = 1.5 Hz), 7.47 (d, 2H, H^3_{Pyr}, J = 7.3 Hz), 7.21 (t, 1H, H^5_{Pyr}, J = 6.4 Hz), thiomethyl protons δ 4.22 (bs, 4H, S(CH_2−Pyr)$_2$), methyl protons δ 0.90 (s, 3H, Pd−CH_3). IR: $\nu_{C=N\ coordinated}$ 1589.3, $\nu_{C=N\ uncoordinated}$ 1602.7 cm^{-1} (KBr). Anal. Calcd for $C_{13}H_{15}ClN_2PdS$: C, 41.84; H, 4.05; N, 7.51. Found: C, 42.08; H, 3.79; N, 7.78.

[Pd(Me)(S−N−S(Me))]OTf (2a). To a solution of 150 mg (0.42 mmol) of [Pd(Me)(S−N−S(Me))]Cl in CH_2Cl_2 (20 mL) was added 113.6 mg (0.44 mmol) of AgOTf. The resulting suspension was stirred in the dark for 3 h and filtered on a Millipore filter. The clear solution obtained was treated with activated charcoal and filtered on Celite filter. Reduction under reduced pressure and addition of diethyl ether yielded the title compound as a whitish solid, which was recrystallized from CH_2Cl_2/diethyl ether and dried under vacuum. A total of 0.28 mmol of the product were obtained (129.3 mg, 67%). ^{1}H NMR ($CDCl_3$, 298 K, ppm): pyridine protons δ 7.92 (t, 1H, H^4_{Pyr}, J = 7.9 Hz), 7.66 (d, 2H, H^3_{Pyr}, H^5_{Pyr}, J = 7.9 Hz), thiomethyl protons δ 4.83 (bs, 4H, Pyr−CH_2−S), methyl protons δ 2.72 (s, 6H, S−CH_3), 0.62 (s, 3H, Pd−CH_3). ^{13}C NMR ($CDCl_3$, 298 K, ppm): pyridine carbons δ 156.31 (C^2_{Pyr}, C^6_{Pyr}), 140.80 (C^4_{Pyr}), 123.33 (C^3_{Pyr}, C^5_{Pyr}), thiomethyl carbons δ 49.98 (S−CH_2−Pyr), methyl carbons δ −8.92 (Pd−CH_3). IR: $\nu_{C=N}$ 1597.0, ν_{C-F} 1257.5, $\nu_{S=O}$ 1029.9 cm^{-1} (KBr). Anal. Calcd for $C_{11}H_{16}F_3NO_3PdS_3$: C, 28.12; H, 3.43; N, 2.98. Found: C, 28.06; H, 3.50; N, 2.73.

The following complexes were synthesized in the same way as [Pd(Me)(S−N−S(Me))]OTf using the appropriate starting substrate.

[Pd(Me)(S−N−S(*t*-Bu))]OTf (2b). Yield: 88% (whitish microcrystals). ^{1}H NMR ($CDCl_3$, 298 K, ppm): pyridine protons δ 7.92 (t, 1H, H^4_{Pyr}, J = 7.5 Hz), 7.82 (d, 2H, H^3_{Pyr}, H^5_{Pyr}, J = 7.5 Hz), thiomethyl protons δ 4.77 (s, 4H, Pyr−CH_2−S), *tert*-butyl protons δ 1.49 (s, 18H, S−C(CH_3)$_3$), methyl protons δ 0.77 (s, 3H, Pd−CH_3). ^{13}C NMR ($CDCl_3$, 298 K, ppm): pyridine carbons δ 157.35 (C^2_{Pyr}, C^6_{Pyr}), 140.57 (C^4_{Pyr}), 122.62 (C^3_{Pyr}, C^5_{Pyr}), thioether carbons δ 54.06 (S-*C*(CH$_3$)$_3$), 44.79 (S−CH_2−Pyr), *tert*-butyl carbons δ 31.04 (S−C(*C*H$_3$)$_3$), methyl carbon δ −8.98 (Pd−CH_3). IR: $\nu_{C=N}$ 1595.1, ν_{C-F} 1263.3, $\nu_{S=O}$ 1028.0 cm^{-1} (KBr). Anal. Calcd for $C_{17}H_{28}F_3NO_3PdS_3$: C, 36.81; H, 4.98; N, 2.28. Found: C, 36.81; H, 4.98; N, 2.28.

[Pd(Me)(S−N−S(Ph))]OTf (2c). Yield: 89% (whitish microcrystals). ^{1}H NMR ($CDCl_3$, 298 K, ppm): pyridine and phenyl protons δ 7.94 (d, 1H, H^4_{Pyr}, J = 7.7 Hz), 7.77 (m, 4H, H_{meta}), 7.69 (d, 2H, H^3_{Pyr}, H^5_{Pyr}, J = 7.7 Hz), 7.46 (m, 6H, H_{ortho}, H_{para}), thiomethyl protons δ 5.17 (bs, 4H, Pyr−CH_2−S), methyl protons δ 0.67 (s, 3H, Pd−CH_3). ^{13}C NMR ($CDCl_3$, 298 K, ppm): pyridine carbons δ 156.17 (C^2_{Pyr}, C^6_{Pyr}), 140.58 (C^4_{Pyr}), 123.19 (C^3_{Pyr}, C^5_{Pyr}), phenyl carbons δ 132.56, 131.40, 130.78, 130.28, thiomethyl carbons δ 53.98 (S−CH_2−Pyr), methyl carbon δ −5.63 (Pd−CH_3). IR: $\nu_{C=N}$ 1597.0, ν_{C-F} 1271.0, $\nu_{S=O}$ 1029.9 cm^{-1} (KBr). Anal. Calcd for $C_{21}H_{20}F_3NO_3PdS_3$: C, 42.46; H, 3.39; N, 2.36. Found: C, 42.56; H, 3.68; N, 2.51.

[Pd(Me)(N−S−N)]OTf (5). Yield: 97% (pale orange microcrystals). ^{1}H NMR ($CDCl_3$, 298 K, ppm): pyridine protons δ 8.41 (d, 2H, H^6_{Pyr}, J = 4.6 Hz), 7.96 (td, 2H, H^4_{Pyr}, J = 7.6 Hz, J = 1.5 Hz), 7.58 (d, 2H, H^3_{Pyr}, J = 7.9 Hz), 7.48 (t, 2H, H^5_{Pyr}, J = 6.4 Hz), thiomethyl protons δ 5.18, δ = 4.69 (AB system, 4H, Pyr−CH_2−S, J = 14.9 Hz), methyl protons δ 1.36 (s, 3H, Pd−CH_3). IR: $\nu_{C=N}$ 1602.8, ν_{C-F} 1259.5, $\nu_{S=O}$ 1029.9 cm^{-1} (KBr). Anal. Calcd for $C_{14}H_{15}F_3N_2O_3PdS_2$: C, 34.44; H, 3.05; N, 5.90. Found: C, 34.44; H, 3.05; N, 5.90.

The allyl complexes **3** and **6** were prepared analogously to the similar species whose synthetic procedure was published elsewhere.[4d,8]

[Pd(η^3-1,1,2-(Me)$_3$C$_3$H$_2$)(S−N−S(Me))]OTf (3a). Yield: 90% (cream-colored microcrystals). ^{1}H NMR ($CDCl_3$, 298 K, ppm): pyridine protons δ 7.89 (t, 1H, H^4_{pyr}, J = 7.7 Hz), 7.56 (d, 2H, H^5_{pyr}, H^3_{pyr}, J = 7.7 Hz), thiomethyl protons δ 4.20 (s, 4H, Pyr−CH_2−S), allyl protons δ 3.97 (s, 2H, H_{syn}, H_{anti}), thiomethyl protons δ 2.15 (s, 6H, S−CH_3), allyl methyl δ 2.14 (s, 3H, C^2-CH_3), 1.69 (bs, 3H, C^1−CH_{3syn}), 1.50 (bs, 3H, C^1−CH_{3anti}). IR $\nu_{C=N}$: 1597.0 cm^{-1} (KBr). Anal. Calcd for $C_{16}H_{24}F_3NO_3PdS_3$: C, 35.72; H, 4.50; N, 2.60. Found: C, 35.72; H, 4.68; N, 2.83.

[Pd(η^3-1,1,2-(Me)$_3$C$_3$H$_2$)(S−N−S(*t*-Bu))]OTf (3b). Yield: 87.4% (yellow microcrystals). ^{1}H NMR ($CDCl_3$, 298 K, ppm): pyridine protons δ 7.87 (t, 1H, H^4_{pyr}, J = 7.8 Hz), 7.61 (d, 2H, H^5_{pyr}, H^3_{pyr}, J = 7.8 Hz), thiomethyl protons δ 4.24 (s, 4H, Pyr−CH_2−S), allyl protons δ 4.10 (bs, 2H, H_{syn}, H_{anti}), allyl methyl δ 2.16 (s, 3H, C^2−CH_3), 1.74 (s, 3H, C^1−CH_{3syn}), 1.51 (s, 3H, C^1−CH_{3anti}), *tert*-butyl protons δ 1.32 (s, 18H, S−C(CH_3)$_3$). IR $\nu_{C=N}$: 1602.8 cm^{-1} (KBr). Anal. Calcd for $C_{22}H_{36}F_3NO_3PdS_3$: C, 42.47; H, 5.83; N, 2.25. Found: C, 42.65; H, 5.86; N, 2.47.

[Pd(η^3-1,1,2-(Me)$_3$C$_3$H$_2$)(S−N−S(Ph))]OTf (3c). Yield: 73.2% (whitish microcrystals). ^{1}H NMR ($CDCl_3$, 298 K, ppm): pyridine and phenyl protons δ 7.55 (t, 1H, H^4_{pyr}, J = 7.7 Hz), 7.22 (m, 12H, H^5_{pyr}, H^3_{pyr}, S−C_6H_5), thiomethyl protons δ 4.15 (s, 4H, Pyr−CH_2−S), allyl protons δ 4.13 (bs, 2H, H_{syn}, H_{anti}), allyl methyl δ 2.17 (s, 3H, C^2−CH_3), 1.68 (s, 3H, C^1−CH_{3syn}), 1.46 (s, 3H, C^1−CH_{3anti}). IR $\nu_{C=N}$: 1603.0 cm^{-1} (KBr). Anal. Calcd for $C_{26}H_{28}F_3NO_3PdS_3$: C, 47.16; H, 4.26; N, 2.12. Found: C, 47.34; H, 3.96; N, 1.84.

[Pd(η^3-1,1,2-(Me)$_3$C$_3$H$_2$)(N−S−N)]ClO$_4$ (6). Yield: 54.8% (red-orange microcrystals). ^{1}H NMR ($CDCl_3$, 298 K, ppm): pyridine protons δ 8.44 (d, 2H, H^6_{pyr}, J = 4.2 Hz), 7.66 (td, 2H, H^4_{pyr}, J = 7.5 Hz, J = 1.7 Hz), 7.21(d, 2H, H^3_{pyr}, J = 6.22 Hz), 7.19 (t, 2H, H^5_{pyr}, J = 6.2), thiomethyl protons δ 4.37 (s, 4H, Pyr−CH_2−Ss), allyl protons δ 4.08 (s, 1H, H_{syn}), 3.71 (s, 1H, H_{anti}), allyl methyl δ 2.17 (s, 3H, C^2−CH_3), 1.70 (s, 3H, C^1−CH_{3syn}), 1.46 (s, 3H, C^1−CH_{3anti}). IR $\nu_{C=N}$: 1602.8 cm^{-1} (KBr). Anal. Calcd for $C_{18}H_{23}ClN_2O_4PdS$: C, 42.78; H, 4.59; N, 5.54. Found: C, 42.74; H, 4.72; N, 5.33.

X-ray Analysis. The X-ray data collection of [Pd(Me)(S−N−S(*t*-Bu))]OTf (**2b**) was performed at room temperature with a STADI 4 CCD STOE area detector diffractometer on single crystal mounted in a thin-walled glass capillary with graphite-monochromated Mo Kα radiation (λ = 0.71073 Å). Systematic absences could not unambiguously identify the space group; solution was therefore carried out in *C*2, *Cm*, and *C*2/*m*. Close scrutiny of the possible monoclinic space group with mirror planes yielded no viable solutions, while a satisfactory refinement was achieved in the first space group. However, solution in *C*2 of the structures performed with the SHELXTL/PC[11] was rather difficult due to the pseudo mirror plane bisecting the cationic complex. The metal and the two sulfur atoms were located from a Patterson synthesis, while the sulfonato group and most of the non hydrogen atoms were identified from a subsequent Fourier synthesis. After some cycles of refinement, performed with the SHEXL-93 program,[12] the SO_3 group appeared disordered, two distinct sites for oxygen atoms being identified, and these were refined satisfactorily with occupan-

(11) Sheldrick, G. M. *SHELXTL/PC*, Version 5.03; Siemens Analytical X-ray Instruments Inc.: Madison, WI, 1994.
(12) Sheldrick, G. M. *SHELXL-93*, Program for the Refinement of Crystal Structures; University of Göttingen: Germany, 1993.

Table 3. Equilibrium Constants (K_E) for the Addition of Chloride to Complexes I (Scheme 2) in CD_2Cl_2 at 298 K and Second-Order Rate Constants

complex **I**	K_E[a]	k_I (mol^{-1} dm^3 s^{-1})
[Pd(Me)(S−N−S(Ph))]$^+$	780 ± 140	(4.35 ± 0.09) × 10^{-4} [b]
[Pd(Me)(S−N−S(Me))]$^+$	53 ± 7	∼ 8 × 10^{-6} [c]
[Pd(Me)(S−N−S(*t*-Bu))]$^+$	71 ± 14	∼ 1 × 10^{-6} [c]
[Pd(Me)(N−S−N)]$^+$		fast

complex **II**	k_{II} (mol^{-1} dm^3 s^{-1})[d]	k_2 (mol^{-1} dm^3 s^{-1})
[PdCl(Me)(S−N−S(Ph))]	80 ± 2	23−164[e]
[PdCl(Me)(S−N−S(Me))]	36 ± 1	2.42−117[e]
[PdCl(Me)(S−N−S(*t*-Bu))]	0.4 ± 0.2	0.33 − 30[e]
[PdCl(Me)(N−S−N)]	(4.3 ± 0.2) × 10^{-3}	8.17 × 10^{-4} to 4.0 × 10^{-2} [f]

[a] Determined by ^{1}HNMR technique. [b] Determined by ^{1}H NMR technique under second-order conditions. [c] Determined from $t_{1/2}$ data according to the relationship $k_I = \ln((2[DMA]_0 - [complex]_0)/[DMA]_0)/(([DMA]_0 - [complex]_0)t_{1/2})$. [d] Determined by UV/vis technique from experiments under pseudo-first-order conditions. [e] k_2 values for insertion of DMA into the Pd−Me bond of the complexes [PdCl(Me)(R′N−SR)] (R′N−SR bidentate pyridylthioether ligand bearing an R′ substituent in position 6 of pyridine ring; R′ = Me (lower limit), R′ = Cl (upper limit)). From refs 1a,b. [f] k_2 values for insertion reaction of DMA into the Pd−Me bond of the complexes [PdCl(Me)(HN−SR)] (HN−SR bidentate pyridylthioether ligand without a substituent in the pyridine ring; R = Me (lower limit), R′ = Ph (upper limit)). From refs 1a,b. Second-order rate constants for the reaction of allene (DMA) insertion into the Pd−Me bond of complexes **I** (k_I, in CD_2Cl_2) and **II** (k_{II}, in CH_2Cl_2) (Scheme 4) at 298 K along with second-order rate constants (k_2) for the reactions of allene (DMA) insertion into the Pd−Me bond of related bidentate systems (see Results and Discussion).

cies 2/3 and 1/3. On the contrary, although a final difference Fourier synthesis had shown rather extended regions of electron density at the sites of F atoms, it did not prove possible to resolve them into separate components. In the refinement procedure, based on F^2, only the non-hydrogen atoms of the "inner core", together with the S(3) of the anion, were assigned anisotropic displacement parameters.

As expected, significant matrix correlations (up to 0.89) were observed between thermal motion parameters of the atoms related by the pseudo-mirror (for example, S(1)/S(2), C(2)/C(8), C(3)/C(7), ..., for which *x*, *y*, *z* coordinates correspond with values very close to *x*, −*y*, *z*).

Crystal data, summary of data collection, and structure refinement are collected in Table 4.

Because of pseudosymmetry, which caused problems in refinement, some caution is required in considering the bond lengths and angles.

The X-ray data collection of [Pd(Me)(S−N−S(*t*-Bu))]Cl (**1b**) was performed at 183 K with a Bruker Smart CCD diffractometer on single crystal mounted on a thin-walled glass capillary with graphite-monochromated Mo Kα radiation. All non-H atoms were refined anisotropically. H atoms bound to C atoms were added in calculated positions. The water molecules was refined with site occupancy 0.5. The computer program SHELXTL[11] was used for structure solution and refinement.

Crystal data, summary of data collection, and structure refinement are also collected in Table 4.

Solvents and Reagents. Unless otherwise stated, all the reactions were performed under inert atmosphere (N_2) by Schlenk technique at room temperature. THF and CH_2Cl_2 were dried and distilled on Na/benzophenone and on CaH_2, respectively. Acetone and CH_3CN were stored over molecular sieves and distilled under N_2 immediately before use. All other chemicals were commercially available grade products.

IR, NMR, and UV−Vis Measurements. The IR and ^{1}H and $^{13}C\{^1H\}$ NMR spectra were recorded on a Nicolet Magna 750 spectrophotometer and on a Bruker 300 Avance spectrometer, respectively. UV−vis spectra and kinetic measurements were performed on a Perkin-Elmer Lambda 40 spectrophotometer equipped with a Perkin-Elmer PTP 6 (Peltier Temperature Programmer) apparatus.

Table 4. Crystallographic Data

formula	$C_{17}H_{28}F_3NO_3PdS_3$	$C_{17.5}H_{32}Cl_4N_1O_{0.5}Pd_1S_2$
space group	*C*2 (No. 5)	*Pbcn* (No. 60)
fw	553.98	576.76
a, Å	21.541(4)	28.332(1)
b, Å	12.051(2)	9.5796(4)
c, Å	8.919(2)	18.3486(8)
β, deg	97.15(3)	
V, Å^3	2297(1)	4979.9(4)
Z	4	8
λ Å; *μ*(Mo Kα), mm^{-1}	0.71073; 1.12	0.71073; 1.348
f(calcd), g cm^{-3}	1.602	1.539
no. of indep reflns	3417	6617
no. of reflns with $I>2\sigma(I)$	2221	4058
no. of variables	171	240
R^a	0.048	0.048
wR_2^b	0.100	0.092
largest difference peak (e Å^{-3})	0.60	0.79

[a] $R = \sum||F_o| - |F_c|| / \sum|F_o|$. [b] $wR_2 = [\sum w(F_o^2 - F_c^2)^2 / \sum w(F_o^2)^2]^{1/2}$.

Equilibrium and Kinetic Measurements. The determination of equilibrium constants (Scheme 2) was achieved by adding preweighed aliquots of TEBA chloride (triethylbutylammonium chloride) to a solution in CD_2Cl_2 of the complex under study ([Pd(Me)(S−N−S(R))]OTf, R = Me, *t*-Bu, Ph; $[Pd]_0 \approx 5 \times 10^{-2}$ mol dm^{-3}) into a 5 mm NMR tube at 298 K. The resulting ^{1}H NMR spectra were recorded and analyzed by a nonlinear least-squares procedure according to the following model:

$$[Pd]_0 = [\mathbf{I}] + [\mathbf{II}]$$

$$[Cl^-]_0 = [\mathbf{II}] + [Cl^-]$$

$$K_E = [\mathbf{II}]/[\mathbf{I}][Cl^-]$$

and minimizing the sum of squares

$$\Phi = \sum(\nu_{obs} - \nu_{calc})^2$$

where ν_{obs} is the observed chemical shift upon addition of Cl^- and $\nu_{calc} = \nu_{\mathbf{I}}(1 - [\mathbf{II}]/[Pd]_0) + \nu_{\mathbf{II}}[\mathbf{II}]/[Pd]_0$ is the chemical shift calculated at the current values of the parameters being optimized (K_E and $\nu_{\mathbf{II}}$). $\nu_{\mathbf{I}}$ and $\nu_{\mathbf{II}}$ are the chemical shifts relating to Pd−CH_3 (R = Ph) or CH_2−S (R = Me, *t*-Bu) in **I** and **II**, respectively. During each iterative cycle $\nu_{\mathbf{II}}$ can be held constant at the value experimentally determined from the ^{1}H NMR spectrum of species **II** taken in the presence of excess Cl^-.

The kinetics of DMA insertion were carried out under pseudo-first-order conditions ($[Pd]_0 \approx 10^{-4}$, $[Cl^-]_0 \approx 10^{-3}$, [DMA] > 10^{-3} mol dm^{-3}) in CH_2Cl_2 at 25 °C by adding appropriate aliquots of DMA solutions to solutions of the palladium substrates **II** and TEBA chloride in the prethermostated cell of the spectrophotometer. The kinetics obeyed the monoexponential rate law $A_t = A_\infty + (A_0 - A_\infty)\exp(-k_{obs}t)$, where k_{obs} is given by the expression

$$k_{obs} = [DMA]_0(k_{\mathbf{II}}[Cl^-]_0 + k_{\mathbf{I}}/K_E)/(1/K_E + [Cl^-]_0)$$

according to Scheme 4.

Since $k_{\mathbf{I}}/K_E \ll k_{\mathbf{II}}[Cl^-]_0$ under our experimental condition (see Table 3), k_{obs} reduces to

$$k_{obs} = [DMA]_0 k_{\mathbf{II}}[Cl^-]_0/(1/K_E + [Cl^-]_0)$$

from which the second-order rate constant $k_{\mathbf{II}}$ can be determined from the slope of k_{obs} versus $[DMA]_0$ at the known values of $[Cl^-]_0$ and K_E.

Owing to the small values of $k_{\mathbf{I}}$, these constants were determined by ^{1}H NMR experiments by reacting the chloride-free species **I** ($[\mathbf{I}]_0 \approx 3 \times 10^{-2}$ mol dm^{-3}) with DMA ($[DMA]_0 \approx 0.15$ mol dm^{-3}) and computing the ensuing $k_{\mathbf{I}}$ constants from the customary second-order rate law or from the estimated half-life time as $k_{\mathbf{I}} \approx \ln((2[DMA]_0 - [Pd]_0)/[DMA]_0)/(([DMA]_0 - [Pd]_0)t_{1/2})$.

Supporting Information Available: Text giving details of the X-ray crystal structure studies and table of crystal structure determination data, atomic coordinates, anisotropic thermal parameters, and bond lengths and angles (CIF files) is available free of charge via the Internet at http://pubs.acs.org.

OM030293F